Structure and electrical properties of $K_{0.5}Na_{0.5}NbO_3$–$LiSbO_3$ lead-free piezoelectric ceramics

Dunmin Lin,[a)] K. W. Kwok, K. H. Lam, and H. L. W. Chan
Department of Applied Physics, The Hong Kong Polytechnic University, Kowloon, Hong Kong, China
and Materials Research Centre, The Hong Kong Polytechnic University, Kowloon, Hong Kong, China

Lead-free piezoelectric ceramics $(1-x)K_{0.5}Na_{0.5}NbO_3$–$xLiSbO_3$ have been fabricated by a conventional ceramic sintering technique. The results of x-ray diffraction suggest that Li^+ and Sb^{5+} diffuse into the $K_{0.5}Na_{0.5}NbO_3$ lattices to form a solid solution with a perovskite structure. The ceramics can be well sintered at 1070–1110 °C. The introduction of $LiSbO_3$ into the $Na_{0.5}K_{0.5}NbO_3$ solid solution decreases slightly the paraelectric cubic-ferroelectric tetragonal phase transition temperature (T_c), but greatly shifts the ferroelectric tetragonal-ferroelectric orthorhombic phase transition (T_{O-F}) to room temperature. Coexistence of the orthorhombic and tetragonal phases is formed at $0.05 < x < 0.07$ at room temperature, leading to a significant enhancement of the piezoelectric properties. For the ceramic with $x = 0.06$, the piezoelectric properties become optimum: piezoelectric constant $d_{33} = 212$ pC/N, planar and thickness electromechanical coupling factors $k_P = 46\%$ and $k_t = 47\%$, respectively, remanent polarization $P_r = 15.0$ $\mu C/cm^2$, coercive field $E_c = 1.74$ kV/mm, and Curie temperature $T_C = 358$ °C. © *2007 American Institute of Physics.*
[DOI: 10.1063/1.2715486]

I. INTRODUCTION

Piezoelectric ceramics based on lead zirconate titanate (abbreviated as PZT) are widely used in actuators and sensors as well as microelectronic devices due to their superior piezoelectric and electrical properties. However, the use of lead-based ceramics has caused serious environmental problems because of the high toxicity of lead oxide and its high vapor pressure during sintering. Therefore, there is a great need to develop lead-free piezoelectric ceramics with excellent piezoelectric properties for replacing the lead-containing ceramics in various applications. Several lead-free piezoelectric ceramics such as $Bi_{0.5}Na_{0.5}TiO_3$-based materials,[1–4] Bi-layered structure materials,[5,6] tungsten bronze-type materials,[7] $BaTiO_3$-based ceramics,[8] and alkaline niobate-based materials[9–21] have been extensively investigated. An important progress of grain-oriented alkaline niobate-based ceramics has been reported recently[22] and piezoelectric ceramics should be "lead-free at last."[23]

Among the lead-free ceramics, $K_{0.5}Na_{0.5}NbO_3$ (abbreviated as KNN), the solid solution of ferroelectric $KNbO_3$ and antiferroelectric $NaNbO_3$, is considered one of the most promising candidates for lead-free piezoelectric ceramics because of its very high Curie temperature (above 400 °C), good ferroelectric properties ($P_r = 33$ $\mu C/cm^2$), and large electromechanical coupling factors. However, it is very difficult to obtain dense and well-sintered KNN ceramics using an ordinary sintering process because of the volatility of alkaline elements at high temperatures. For a well-sintered KNN ceramic (e.g., prepared by hot-pressing technique), it possesses good piezoelectric properties ($d_{33} = 160$ pC/N, $k_P = 45\%$) and high density ($\rho = 4.46$ g/cm^3).[10] However, there is a severe degradation in piezoelectric properties (d_{33}

$= 80$ pC/N, $k_P = 36\%$) and density ($\rho = 4.25$ g/cm^3) for an air-fired KNN ceramics.[9,12] A number of studies have been carried out to improve the properties of KNN ceramics; these include the formation of solid solutions of KNN with other ferroelectrics or nonferroelectrics, e.g., KNN–$LiNbO_3$,[13] KNN–$BaTiO_3$,[16] KNN–$SrTiO_3$,[14,15] KNN–$LiTaO_3$,[24] and KNN–$Li(Nb,Ta,Sb)O_3$,[22] as well as the use of sintering aids, e.g., $K_{5.4}Cu_{1.3}Ta_{10}O_{29}$.[18,19]

On the basis of the reported work and the analogy of PZT-based ceramics, it is noted that the key approach for improving the piezoelectric properties of KNN-based ceramics is to lower the ferroelectric tetragonal-ferroelectric orthorhombic phase transition (T_{O-F}), forming coexistence of the tetragonal and orthorhombic phases at room temperature. This could be achieved by partial substitutions of A-site ions $(Na_{0.5}K_{0.5})^+$ and B-site ion Nb^{5+} by other analogous ions in the ABO_3-type (KNN) perovskite structure. In the present work, KNN ceramics partially substituted with Li^+ and Sb^+ were prepared by ordinary solid-state sintering, and their structure, piezoelectric, dielectric, and ferroelectric properties were studied. The effects of the substitutions on the phase transition were also investigated.

II. EXPERIMENT

$(1-x)K_{0.5}Na_{0.5}NbO_3$–$xLiSbO_3$ ceramics were prepared by a conventional ceramic fabrication technique using analytical-grade metal oxides or carbonate powders: Na_2CO_3 (99.8%), K_2CO_3 (99.9%), Li_2CO_3 (99%), Sb_2O_5 (99%), and Nb_2O_5 (99.95%). The powders in the stoichiometric ratio of the compositions were mixed thoroughly in ethanol using zirconia balls for 8 h, and then dried and calcined at 880 °C for 6 h. After the calcination, the mixture was ball milled again and mixed thoroughly with a polyvinyl alcohol (PVA) binder solution and then pressed into disk samples. The disk

a)Electronic mail: ddmd222@yahoo.com.cn

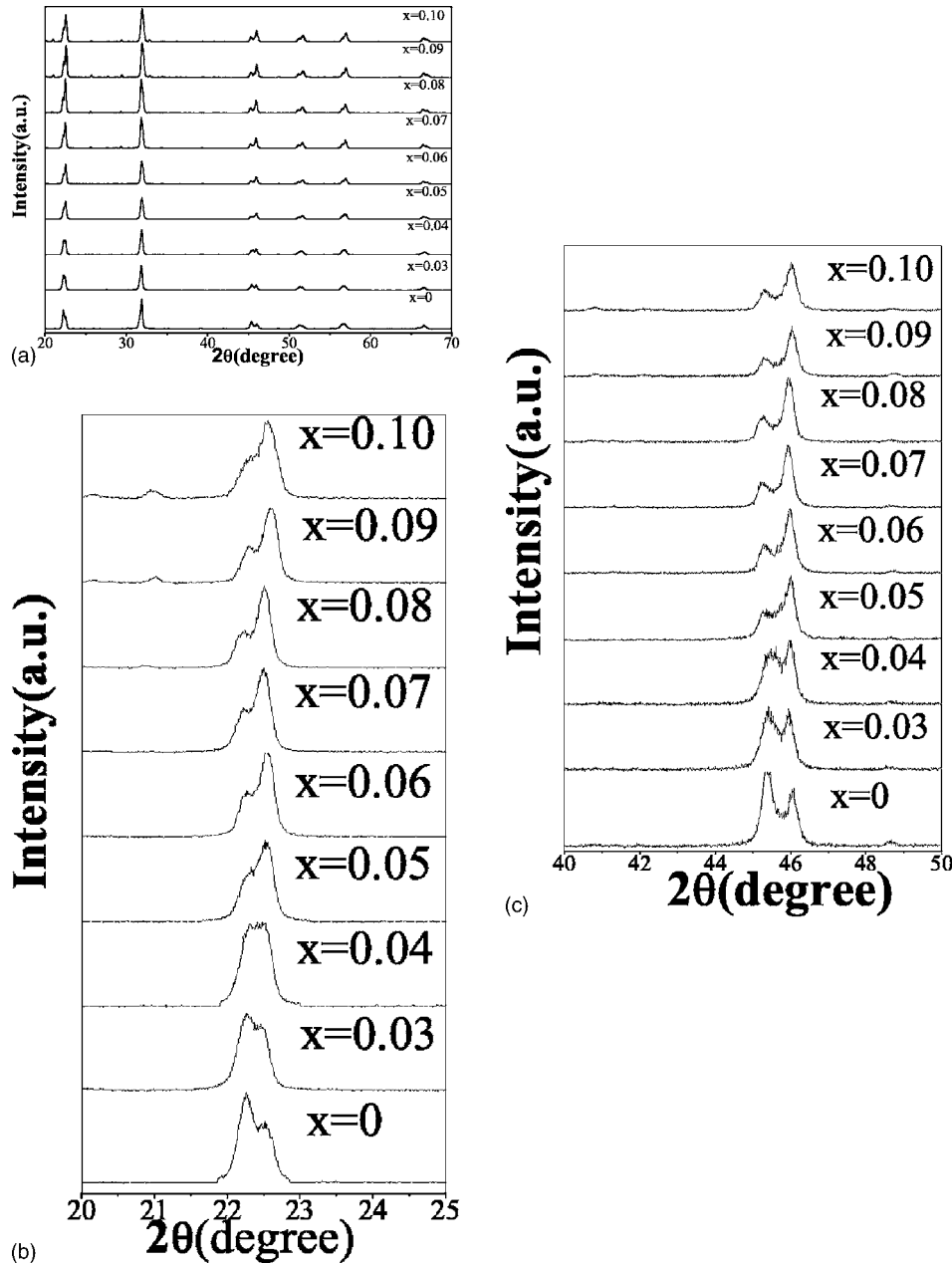**101**, 074111-1

FIG. 1. X-ray diffraction patterns of the $(1-x)K_{0.5}Na_{0.5}NbO_3-xLiSbO_3$ ceramics in the ranges of 2θ (a) from 20° to 70°, (b) from 21.5° to 23.5°, and (c) from 44° to 47°.

samples were finally sintered at 1070–1110 °C for 4 h in air. Silver electrodes were applied on the top and bottom surfaces of the samples for the subsequent poling and measurements.

The crystallite structure of the sintered samples was examined using x-ray diffraction (XRD) analysis with Cu $K\alpha$ radiation (Bruker D8 Advance). The microstructures were observed using a scanning electron microscope (Leica Stereoscan 440). The bulk densities ρ were measured by Archimedes' method. The dielectric constant ε and loss tangent tan δ at 1, 10, and 100 kHz of the ceramics were measured as a function of temperature using an impedance analyzer (HP 4192A). A conventional Sawyer-Tower circuit was used to measure the polarization hysteresis (P-E) loop at 100 Hz. The electromechanical coupling factors k_P and k_t were determined by the resonance method according to the IEEE Standard 176 using an impedance analyzer (HP 4294A). The piezoelectric constant d_{33} was measured using a

piezo-d_{33} meter (ZJ-3A, China). Prior to the k and d_{33} measurements, the ceramics were poled under a dc field of 4–5 kV/mm at 180 °C in a silicone oil bath for 30 min.

III. RESULTS AND DISCUSSION

Figure 1(a) shows the XRD patterns of the $(1-x)K_{0.5}Na_{0.5}NbO_3-xLiSbO_3$ ceramics with $0 \leqslant x \leqslant 0.10$. It can be seen that a single-phase perovskite structure was formed in the ceramics with $x \leqslant 0.06$. As the crystal structure of KNN (perovskite structure) is very different from $LiSbO_3$ (ilmenite structure),[25] our results suggest that Li$^+$ and Sb^{5+} have diffused into the KNN lattices, with Li$^+$ entering the $(Na_{0.5}K_{0.5})^+$ sites and Sb^{5+} occupying the Nb^{5+} sites, to form a homogeneous solid solution. For the ceramics with $x \geqslant 0.07$, a small amount of secondary phase $K_3Li_2Nb_5O_{15}$ with the tetragonal tungsten bronze structure is formed. Figures 1(b) and 1(c) show the enlarged XRD patterns of the

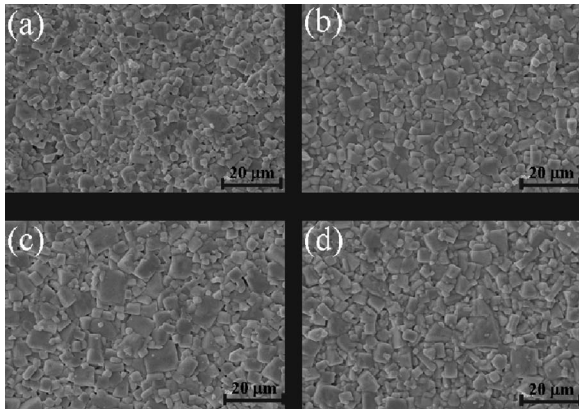FIG. 2. SEM micrographs of the $(1-x)K_{0.5}Na_{0.5}NbO_3-xLiSbO_3$ ceramics: (a) $x=0$, sintered at 1100 °C for 4 h; (b) $x=0.03$, sintered at 1090 °C for 4 h; (c) $x=0.06$, sintered at 1080 °C for 4 h; and (d) $x=0.09$, sintered at 1070 °C for 4 h.

FIG. 3. Densities ρ of the $(1-x)K_{0.5}Na_{0.5}NbO_3-xLiSbO_3$ ceramics as a function of x.

ceramics in the ranges of 2θ from 21.5° to 23.5° and from 44° to 47°, respectively. It can be seen that at $x \leq 0.04$, the ceramic has an orthorhombic perovskite structure (the corresponding XRD patterns can be indexed by Ref. 31). As x (i.e., the concentration of $LiSbO_3$) increases, a tetragonal phase appears and increases continuously. At $x \geq 0.08$, the ceramic becomes possessing the tetragonal phase only (the XRD patterns can be indexed by Ref. 32). These suggest that the (perovskite) orthorhombic and tetragonal phases coexist in the $(1-x)K_{0.5}Na_{0.5}NbO_3-xLiSbO_3$ ceramics with $0.05 < x < 0.07$. Similar to $BaTiO_3$, the orthorhombic phase of the ceramics demonstrates a nonprimitive cell, while the tetragonal phase is primitive. It is also noted that the diffraction peaks shift slightly towards high diffraction angles as x increases. This may be attributed to the smaller ionic radii of Li^+ and Sb^{5+} than those of $(Na_{0.5}K_{0.5})^+$ and Nb^{5+}.

Figure 2 shows the scanning electron microscopy (SEM) micrographs of the $(1-x)K_{0.5}Na_{0.5}NbO_3-xLiSbO_3$ ceramics. For the pure KNN ceramic (i.e., $x=0$), the grains have a diameter in the range of $1-1.5$ μm, and a small amount of pores are observed [Fig. 2(a)]. With the increase of x to 0.03, the grains become slightly larger and more uniform [Fig. 2(b)]. The ceramic is denser and almost no pores are observed. At $x=0.06$, there are distinct grains of diameter about 10 μm uniformly distributed among the grains which are of much smaller diameters, about 1.5 μm [Fig. 2(c)]. The grains become relatively uniform in size again for the ceramic with $x=0.09$ [Fig. 2(d)]. Figure 3 shows the density of the ceramics as a function of x. After the addition of $LiSbO_3$, the density increases and has a high value of $4.216-4.397$ g/cm³ in the range of x from 0.02 to 0.06. The decrease in density at higher x may be attributed to the formation of the secondary phase $K_3Li_2Nb_5O_{15}$ of which the theoretical density is low (4.376 g/cm³).[3]

It is clearly seen that the addition of $LiSbO_3$ can assist the densification of the KNN ceramics and thus improves the sintering performance of the ceramics. Although the sintering temperature decreases with increasing the concentration of $LiSbO_3$, the grain size increases and the ceramics become denser and well sintered more easily. This may be attributed to the low melting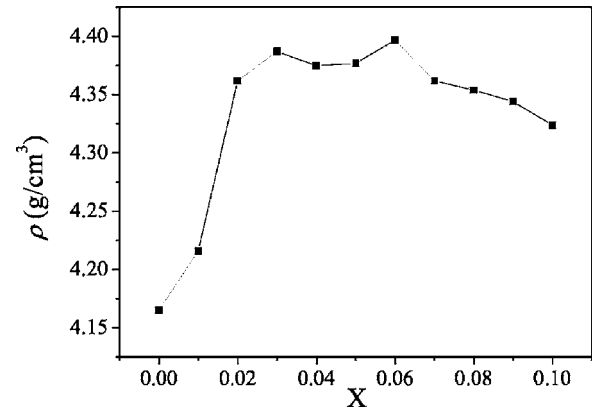 temperature of Li compounds that appears to promote the formation of a liquid phase during sintering. The ceramics can be well sintered at $1070-1110$ °C, which is about 200 °C lower than the sintering temperature for PZT ceramics.

It has been shown that $KNbO_3$ exhibits similar phase transitions as $BaTiO_3$, i.e., transforming from the cubic paraelectric to the tetragonal ferroelectric phase at 435 °C (T_c) and from tetragonal ferroelectric to the orthorhombic ferroelectric phase at 225 °C (T_{O-F}). The phase transitions for the solid solution of $KNbO_3$ with $NaNbO_3$ ($K_{0.5}Na_{0.5}NbO_3$) is similar, but with transition temperatures changed slightly.[26,27] In agreement with the reported work, the observed temperature dependence of the dielectric constant ε for the KNN ceramic shows the two transitions, giving $T_c=421$ °C and $T_{O-F}=226$ °C [Fig. 4(a)]. After the addition of $LiSbO_3$, the ceramics retain the ferroelectric characteristic, with T_C (Curie temperature) shifted to lower temperatures. Figures 4(b)–4(d) show, as examples, the temperature dependences of ε for the $(1-x)K_{0.5}Na_{0.5}NbO_3-xLiSbO_3$ ceramics with $x=0.03$, 0.06, and 0.09. It can be seen that the ceramics also exhibit the tetragonal-orthorhombic phase transition [Figs. 4(b)–4(d)]. Unlike T_c, T_{O-F} decreases much faster with increasing x. For the ceramics with $x \leq 0.06$, the tetragonal-orthorhombic phase transition becomes weak and shifted to temperatures below 100 °C, which is shown clearly in the insets of Figs. 4(c) and 4(d). As there is only a small amount of the secondary phase $K_3Li_2Nb_5O_{15}$ (tetragonal tungsten bronze structure) existing in the ceramics with $x \geq 0.07$, the observed transition peaks should be mainly associated with the transformations between different phases of the perovskite structure.

The variations of T_c and T_{O-F} with x are summarized to form a phase diagram, as shown in Fig. 5. It has been shown that a partial substitution of A-site ions $(Na_{0.5}K_{0.5})^+$ by Li^+ can cause T_c to increase while T_{O-F} to decrease.[13] On the other hand, a partial substitution of B-site ions Nb^{5+} by Ta^{5+} can decrease both T_c and T_{O-F} rapidly.[18,19] Therefore, the cosubstitution of A-site and B-site ions by Li^+ and Sb^{5+}, respectively, may result in different rates of decrease in T_c and T_{O-F}, as in our case shown in Fig. 5. For T_c, the initial rate of decrease (dT/dx) is about 10 °C/mol % at $x \leq 0.06$ and then
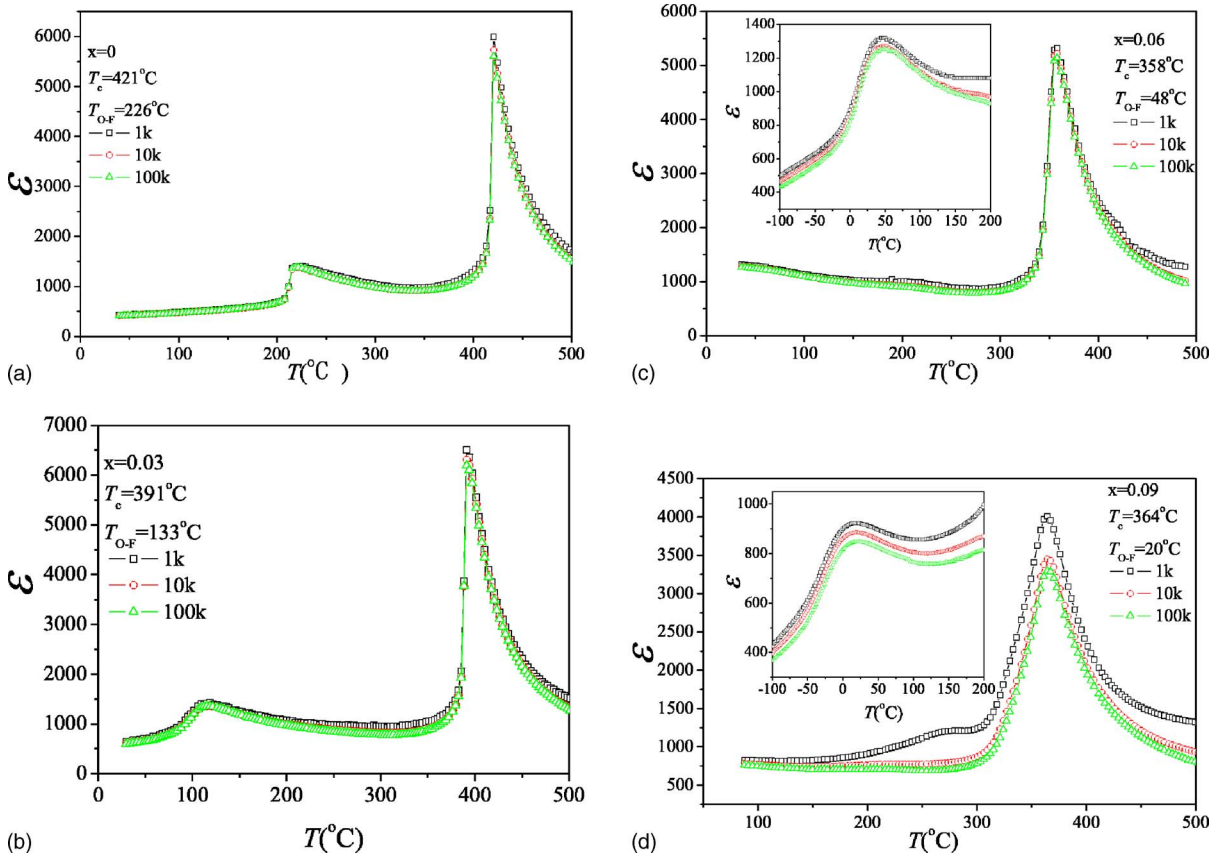
FIG. 4. (Color online) Dielectric constant ε of the $(1-x)K_{0.5}Na_{0.5}NbO_3-xLiSbO_3$ ceramics as a function of temperature: (a) $x=0$, (b) $x=0.03$, (c) $x=0.06$, and (d) $x=0.09$ (the insets show the dependences of ε on temperature T at the range of temperature from -196 to $150\,°C$).

becomes almost zero. Conversely, the initial rate of decrease for T_{O-F} is about $25\,°C/mol\%$ at $x \leq 0.08$; then T_{O-F} increases slightly with increasing x. It can also be seen that the observed T_{O-F} for the ceramics with $x \geq 0.06$ is close to room temperature. This is in agreement with our room-temperature XRD results that the orthorhombic and tetragonal phases coexist in the ceramics with $0.05 < x < 0.07$ (Fig. 1).

Figure 6 shows, as examples, the P-E hysteresis loops of the $(1-x)K_{0.5}Na_{0.5}NbO_3-xLiSbO_3$ ceramics with $x=0$, 0.03, 0.06, and 0.09, while the variations of the remanent polarization P_r and coercive field E_c with x are shown in Fig. 7. All the ceramics exhibit a well-saturated P-E loop under an elec-

tric field of $6-7\,kV/mm$. The pure KNN ceramic has a relatively large P_r ($23.6\,\mu C/cm^2$) and very low E_c ($0.77\,kV/mm$). Nevertheless, because of the poor densification [Fig. 2(a)], the observed P_r of the pure KNN ceramic is smaller than that of a hot-pressed KNN ceramic ($33\,\mu C/cm^2$). After the addition of $LiSbO_3$, P_r decreases with increasing x while E_c increases (Fig. 7). The decrease in P_r suggests that the addition of $LiSbO_3$ would weaken the ferroelectricity of the ceramics. Similar weakening effects
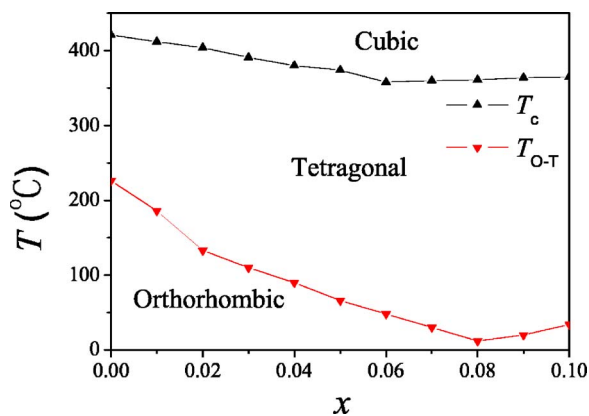

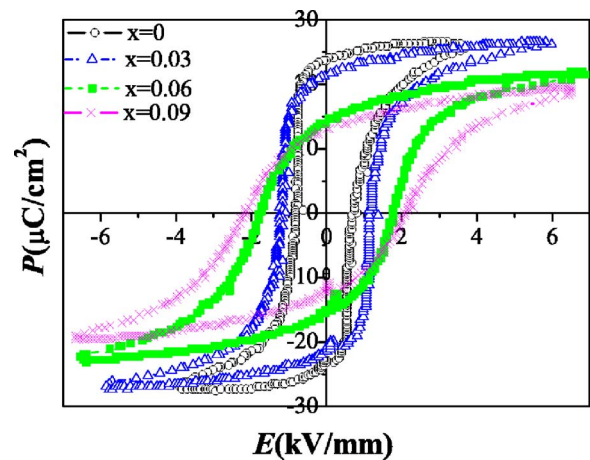FIG. 5. (Color online) Phase diagram of the $(1-x)K_{0.5}Na_{0.5}NbO_3-xLiSbO_3$ with $0 \leq x \leq 0.10$.

FIG. 6. (Color online) P-E hysteresis loops of the $(1-x)K_{0.5}Na_{0.5}NbO_3-xLiSbO_3$ ceramics with different x.

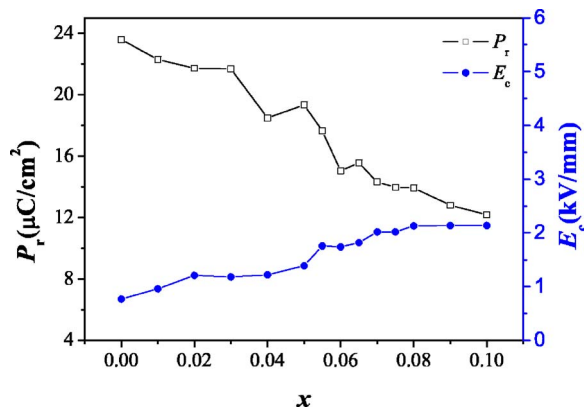FIG. 7. (Color online) Variations of the remanent polarization P_r and coercive field E_c with x for the $(1-x)K_{0.5}Na_{0.5}NbO_3-xLiSbO_3$ ceramics.

FIG. 9. (Color online) Dielectric properties of the $(1-x)K_{0.5}Na_{0.5}NbO_3-xLiSbO_3$ ceramics as a function of the concentration of $LiSbO_3$.

have also been reported for other KNN-based ceramics, such as $(K_{0.5}Na_{0.5})(Nb_{1-x}Ta_x)O_3$,[18] Li-modified KNN ceramics,[28] and KNN–LiTaO$_3$ ceramics.[24]

Figures 8 and 9 show the dependences of the piezoelectric and dielectric properties of the $(1-x)K_{0.5}Na_{0.5}NbO_3-xLiSbO_3$ ceramics on x, respectively. As shown in Fig. 8, the piezoelectric constant d_{33} increases sharply with increasing x and then decreases, giving a maximum value of 212 pC/N at $x=0.06$. Similar to d_{33}, the electromechanical coupling factors k_P and k_t reach a maximum value of 46% and 47%, respectively, at $x=0.06$. The dielectric constant ε also shows similar dependence on x (Fig. 9), while the loss tangent $\tan\delta$ remains almost unchanged. At $x=0.06$, the ceramic has a ε value of 1335 and a $\tan\delta$ value of 2.8%.

It is well known that the morphotropic phase boundary (MPB) plays a very important role in the improvement of piezoelectric properties of perovskite piezoelectric ceramics, such as PZT,[29] $Pb(Mg_{1/3}Nb_{2/3})O_3-PbTiO_3$,[30] $Bi_{0.5}Na_{0.5}TiO_3-BaTiO_3$,[1] and $Bi_{0.5}Na_{0.5}TiO_3-Bi_{0.5}K_{0.5}TiO_3$.[4] In general, the piezoelectric properties of the ceramics become maximum near the MPB region. MPB is defined as an abrupt structural change for a solid solution with variation in composition.[26] The term "morphotropic" means literally "the boundary between two forms." Typically, the change is nearly independent of temperature, giv-
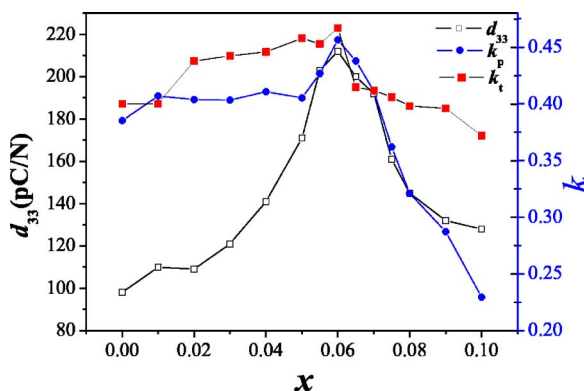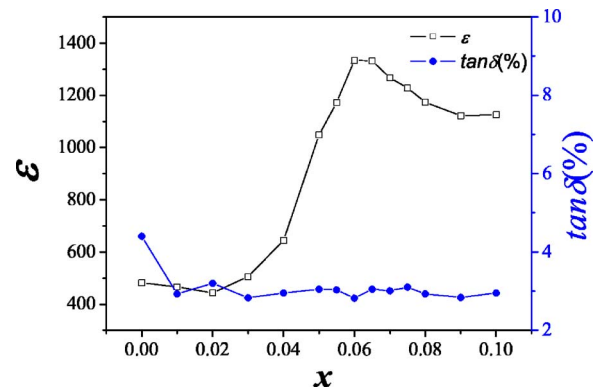
ing a nearly vertical line in the phase diagram such as those for the PZT and lead magnesium niobate-lead titanate (PMN-PT) systems.[29] It is generally believed that the enhancement in piezoelectric properties of the ceramics near the MPB is mainly attributed to the more possible polarization states resulting from the coexistence of the two phases. Unlike PZT and other systems, the phase transitions for the $(1-x)K_{0.5}Na_{0.5}NbO_3-xLiSbO_3$ ceramics depend not only on the compositions but also on the temperature (Fig. 5). Although the phase boundary between the orthorhombic and tetragonal phases may not be a MPB, it is believed to be the major origin for the enhancement in piezoelectric properties of the ceramics. Similar to the other systems with MPB, the ceramics with x in the range of 0.05–0.07 contain both the orthorhombic and tetragonal phases, and thus more possible polarization states. Therefore, although the ceramic with $x=0.06$ possesses a lower P_r as compared to the KNN ceramic (15.0 $\mu C/cm^2$ vs 23.6 $\mu C/cm^2$), it shows the optimum piezoelectric properties ($d_{33}=212$ pC/N, $k_P=46\%$, and $k_t=47\%$). The improvement in densification [Figs. 2(c) and 3] may lead to the enhancement of piezoelectric properties, but it should not be the major reason. On the other hand, although the ceramics with $x=0.07$, 0.08, 0.09, and 0.10 also reside in the region of coexistence, their piezoelectric properties are poorer. This may be caused by the formation of the secondary phase $K_3Li_2Nb_5O_{15}$ in these ceramics (Fig. 1).

IV. CONCLUSIONS

Dense $K_{0.5}Na_{0.5}NbO_3-LiSbO_3$ ceramics have been prepared by a conventional ceramic sintering technique, and a phase diagram for the solid solution $K_{0.5}Na_{0.5}NbO_3-LiSbO_3$ has been established. The ceramic possesses a single-phase perovskite structure at $x\leq0.06$. As the content of $LiSbO_3$ becomes larger (i.e., $x\geq0.07$), a secondary phase $K_3Li_2Nb_5O_{15}$ is formed. The addition of $LiSbO_3$ decreases the sintering temperature of the ceramics, assists the densification, and shifts the ferroelectric tetragonal-to-ferroelectric orthorhombic phase transition (T_{O-F}) to room temperature. Coexistence of the orthorhombic and tetragonal phases is developed at $0.05<x<0.07$ at room temperature, leading to the significant enhancement of the piezoelectric properties. Nevertheless, the addition of $LiSbO_3$ weakens the ferroelec-

FIG. 8. (Color online) Piezoelectric properties of the $(1-x)K_{0.5}Na_{0.5}NbO_3-xLiSbO_3$ ceramics as a function of the concentration of $LiSbO_3$.

tricity of the ceramics at the same time. For the ceramic with $x=0.06$, the piezoelectric properties become optimum, giving $d_{33}=212$ pC/N, $k_P=46\%$, $k_t=47\%$, and Curie temperature $T_C=358$ °C.

ACKNOWLEDGMENTS

[1]T. Takenaka, K. Maruyama, and K. Sakata, Jpn. J. Appl. Phys., Part 1 **30**, 2236 (1991).
[2]X. Wang, X. G. Tang, and H. L. W. Chan, Appl. Phys. Lett. **85**, 91 (2004).
[3]D. Lin, D. Xiao, J. Zhu, and P. Yu, Appl. Phys. Lett. **88**, 062901 (2006).
[4]A. Sasaki, T. Chiba, Y. Mamiya, and E. Otsuki, Jpn. J. Appl. Phys., Part 1 **38**, 5564 (1999).
[5]R. Jain, A. K. S. Chauhan, V. Gupta, and K. Sreenivas, J. Appl. Phys. **97**, 124101 (2005).
[6]W. Li, J. Gu, C. Song, D. Su, and J. Zhu, J. Appl. Phys. **98**, 114104 (2005).
[7]R. Xie, Y. Akimune, K. Matsuo, T. Sugiyama, N. Hirosaki, and T. Sekiya, Appl. Phys. Lett. **80**, 835 (2002).
[8]Z. Yu, C. Ang, R. Guo, and A. S. Bhalla, J. Appl. Phys. **92**, 1489 (2002).
[9]L. Egerton and D. M. Dillom, J. Am. Ceram. Soc. **42**, 438 (1959).
[10]R. E. Jaeger and L. Egerton, J. Am. Ceram. Soc. **45**, 209 (1962).
[11]R. H. Dungan and R. D. Golding, J. Am. Ceram. Soc. **48**, 601 (1965).
[12]Z. S. Ahn and W. A. Schulze, J. Am. Ceram. Soc. **70**, 18 (1987).
[13]Y. Guo, K. Kakimoto, and H. Ohsato, Appl. Phys. Lett. **85**, 4121 (2004).
[14]Y. Guo, K. Kakimoto, and H. Ohsato, Solid State Commun. **129**, 279 (2004).
[15]R. Wang, R. Xie, K. Hanada, K. Matsusak, H. Bando, and M. Itoh, Phys. Status Solidi A **202**, R57 (2005).
[16]C. W. Ahn, H. C. Song, S. Nahm, S. H. Park, K. Uchino, S. Priya, H. G. Lee, and N. K. Kang, Jpn. J. Appl. Phys., Part 2 **44**, L1361 (2005).
[17]E. Hollenstein, M. Davis, D. Damjanovic, and N. Setter, Appl. Phys. Lett. **87**, 182905 (2005).
[18]M. Matsubara, K. Kikuta, and S. Hirano, J. Appl. Phys. **97**, 114105 (2005).
[19]M. Matsubara, T. Yamaguchi, W. Sakamoto, K. Kikuta, T. Yogo, and S. Hirano, J. Am. Ceram. Soc. **88**, 1190 (2005).
[20]H. Takao, Y. Saito, Y. Aoki, and K. Horibuchi, J. Am. Ceram. Soc. **89**, 1951 (2006).
[21]R. Zuo, J. Rödel, Re. Chen, and L. Li, J. Am. Ceram. Soc. **89**, 2010 (2006).
[22]Y. Saito, H. Takao, T. Tani, T. Nonoyama, K. Takatori, T. Homma, T. Nagaya, and M. Nakamur, Nature (London) **432**, 84 (2004).
[23]E. Cross, Nature (London) **432**, 24 (2004).
[24]Y. Guo, K. Kakimoto, and H. Ohsato, Mater. Lett. **59**, 241 (2005).
[25]N. Kumada, N. Takahashi, and N. Kinomura, J. Solid State Chem. **126**, 121 (1996).
[26]B. Jaffe, W. R. Cook, and H. Jaffe, *Piezoelectric Ceramics* (Academic, London, 1971), pp. 53–64, 135–183, and 185–194.
[27]M. D. Maeder, D. Damjanovic, and N. Setter, J. Electroceram. **13**, 385 (2004).
[28]M. Matsubara, T. Yamaguchi, K. Kikuta, and S. Hirano, Jpn. J. Appl. Phys., Part 1 **44**, 6136 (2005).
[29]B. Noheda, D. E. Cox, G. Shirane, R. Guo, B. Jones, and L. E. Cross, Phys. Rev. B **63**, 014103 (2000).
[30]B. Noheda, D. E. Cox, G. Shirane, J. Gao, and Z.-G. Ye, Phys. Rev. B **66**, 054104 (2002).
[31]International centre for Diffraction Data, JCPDS-ICDD 2001, file no. 71-2171.
[32]International centre for Diffraction Data, JCPDS-ICDD 2001, file no. 71-0945.